Na silicate and NaPO$_3$ glasses. The Na$^+$ diffusion in SiO$_2$ glass is, therefore, considered as a limiting case where Na$^+$ ions have the highest capability for random (uncorrelated) motion.

References

[1] C. Lim and D. E. Day, "Sodium Diffusion in Glass: I," *J. Am. Ceram. Soc.*, **60** [5–6] 198–203 (1977).

[2] C. Lim and D. E. Day, "Sodium Diffusion in Glass: II," *ibid.*, [11–12] 473–77.

[3] C. Lim and D. E. Day, "Sodium Diffusion in Glass: III," *ibid.*, **61** [3–4] 99–102 (1978).

[4] Y. Haven and J. M. Stevels; pp. 343–47 in IVth International Congress on Glass, Paris, 1956. Imprimerie Chaix, Paris, 1957.

[5] Y. Haven and B. Verkerk, "Diffusion and Electrical Conductivity of Sodium Ions in Sodium Silicate Glasses," *Phys. Chem. Glasses*, **6** [2] 38–45 (1965).

[6] L. W. Barr, J. N. Mundy, and A. H. Rowe; pp. 243–50 in Amorphous Materials. Edited by R. W. Douglas and Bryan Ellis. Wiley-Interscience, New York, 1972.

[7] G. H. Frischat, Ionic Diffusion in Oxide Glasses (Diffusion Monograph Series, No. 3/4). Trans Tech Publications, Bay Village, Ohio, 1975; 182 pp.

[8] A. D. Le Claire; pp. 261–330 in Physical Chemistry, An Advanced Treatise, Vol. 10. Edited by W. Jost. Academic Press, New York, 1970.

[9] N. L. Peterson; pp. 115–70 in Diffusion in Solids: Recent Developments. Edited by A. S. Nowick and J. J. Burton. Academic Press, New York, 1975.

[10] P. G. Shewmon, Diffusion in Solids; pp. 7–11. McGraw-Hill, New York, 1963.

[11] L. W. Barr and A. D. Le Claire, "Correlation Effects in Diffusion," *Proc. Br. Ceram. Soc.*, **1964**, No. 1, pp. 109–28.

[12] J. H. Simmons, "Molecular Stuffing Process for Making High Silica Glasses with Controlled Properties"; unpublished work.

[13] P. B. Macedo, C. T. Moynihan, and R. Bose, "Role of Ionic Diffusion in Polarization in Vitreous Ionic Conductors," *Phys. Chem. Glasses*, **13** [6] 171–79 (1972).

[14] G. H. Frischat, "Sodium Diffusion in Various Vitreous Silicas," *Glastech. Ber.*, **43** [12] 482–88 (1970).

[15] R. H. Doremus, "Electrical Conductivity and Electrolysis of Alkali Ions in Silica Glass," *Phys. Chem. Glasses*, **10** [1] 28–33 (1969).

[16] R. H. Doremus, "Ionic Transport in Amorphous Oxides," *J. Electrochem. Soc.*, **115** [2] 181–86 (1968).

[17] H. M. Garfinkel, "Ion Exchange Properties of Borosilicate Glass Membranes in Molten Salts," *Phys. Chem. Glasses*, **11** [5] 151–58 (1970).

[18] R. Terai and R. Hayami, "Ionic Diffusion in Glasses," *J. Non-Cryst. Solids*, **18** [2] 217–64 (1975).

[19] R. H. Doremus, "Exchange and Diffusion of Ions in Glass," *J. Phys. Chem.*, **68** [8] 2212–18 (1964).

[20] F. Nicolas, F. Beniere, and M. Chemla, "Isotope Effect of Diffusion of ^{22}Na$^+$-^{24}Na$^+$ in NaCl, KCl, and KBr Single Crystals," *J. Phys. Chem. Solids*, **35** [1] 15–23 (1974).

[21] W. M. Jones, "Permeability and Solubility of He^3 and He^4 in Vitreous Silica," *J. Am. Chem. Soc.*, **75**, 3093–96 (1953).

[22] R. C. Frank, D. E. Swets, and R. W. Lee, "Diffusion of Neon Isotopes in Fused Quartz," *J. Chem. Phys.*, **35** [4] 1451–59 (1961).

Solid-Liquid Equilibria in the System Si$_3$N$_4$-AlN-SiO$_2$-Al$_2$O$_3$

I. K. NAIK,*·* L. J. GAUCKLER,* and T. Y. TIEN*

Department of Materials and Metallurgical Engineering, The University of Michigan, Ann Arbor, Michigan 48109

Solid-liquid equilibria at 1750°C and subsolidus phase relations in the system Si$_3$N$_4$-AlN-SiO$_2$-Al$_2$O$_3$ were determined for the composition region bounded by the β-Si$_3$N$_4$ solid solution line and silica-alumina join. X-ray diffraction and optical microscopy were used to determine the phases present in specimens cooled rapidly after equilibration. The extent of a single liquid-phase region and the tie lines for the β-solid solution + liquid field at 1750°C were established from quantitative X-ray diffractometry and lattice parameter measurements of β-solid solutions in equilibrium with liquid. The results were corroborated by optical microscopy and melting behavior observations. A new composition, Si$_{12}$Al$_{18}$O$_{39}$N$_8$, is suggested for the x_1 phase. The lowest melting temperature in the system is $\approx$1480°C and the corresponding composition is 10 eq% Al-90 eq% O.

I. Introduction

CERAMIC materials based on the system Si,Al/N,O are currently being considered as one of the promising candidates for structural application in an energy-efficient gas turbine. Boskovic *et al.*[1] showed that Si$_3$N$_4$-based ceramics can be made by pressureless sintering. Since Si$_3$N$_4$-based materials have significant covalent character in their bond scheme, sintering to high density via solid state diffusion is not possible. Therefore, the alternative possibility of sintering in the presence of a liquid must be considered. For a liquid-phase sintering process, it is necessary to understand the solid-liquid equilibria in this system. Since such information is scarce in the literature, a study of these equilibria was undertaken.

The early work on phase relations in the system Si,Al/N,O concerned the formation and nature of the β-Si$_3$N$_4$-based solid solution (β-*ss*) and other solid phases in the system.[2–4] The first detailed study of subsolidus equilibria was reported by Gauckler *et al.*[5] who found that, at 1760°C, adjacent the SiO$_2$-rich side of the β-*ss* phase, a 2-phase region (liquid + β-*ss*) existed. However, the solid-liquid equilibria were not studied in detail. Land *et al.*[6] reported that liquid in this system was confined to the region close to the SiO$_2$ corner and that there was no region where β-*ss* and liquid coexisted at 1800°C in their product or quasi-equilibrium diagram. They also reported that the x_1 phase does not melt at <1800°C. Layden[7] proposed a tentative liquid-phase field using differential thermal analysis (DTA) and microstructure observations. The liquid field extends from the SiO$_2$ corner and includes the x_1 composition at 1750°C. The x_1 phase reportedly melts at $\approx$1720°C. A large β-*ss* + liquid field is also indicated at 1750°C. Layden had difficulty in getting reasonable signal strengths during melting due to foaming of the liquid at the high temperatures involved. Therefore, an alternative method of quantitative phase analysis by X-ray powder diffractometry on a series of well-selected specimens should prove to be a more reliable method of studying solid-liquid equilibria in this system.

II. Experimental Procedure and Observations

The starting materials used were aluminum nitride,† silicon nitride,‡ alumina,§ and silica.¶ The oxygen contents of the nitrides were considered in making up the compositions. Mixtures of different overall compositions in the region between the β-*ss* line and silica-alumina join were made using aluminum nitride-silica-

Fig. 1. Part of isothermal section of the system Si_3N_4-AlN-SiO_2-Al_2O_3 at 1750°C showing solid-liquid equilibria; β-ss = β-Si_3N_4-based solid solution, M = mullite ($3Al_2O_3 \cdot 2SiO_2$), L = liquid.

alumina, silicon nitride-silica-aluminum nitride, and silicon nitride-aluminum nitride-alumina as starting materials. The first group was the most commonly used since aluminum nitride-containing mixtures equilibrated more readily than silicon nitride-containing mixtures.

The selected compositions were made by milling the requisite amounts of starting materials in a tungsten carbide jar with tungsten carbide balls and high purity methanol (<0.2% water) for 30 to 60 min. It was found that the nitrides (AlN and/or Si_3N_4) are hydrolyzed, and thus pick up oxygen, if a significant amount of water is present in the grinding medium. Therefore, contact with water must be avoided during milling to preserve the overall composition of the as-weighed mixture. Tungsten carbide impurity introduced during milling was <1.5 wt%. The milled mixture was dried in shallow glass disks over a laboratory heater and cold-pressed into a pellet (1.3 cm in diam. by 1.3 cm thick) at 110 MPa. The pellet was put in a boron nitride crucible and, in most cases, packed in powder of the same composition to minimize weight loss in the pellet during firing.

Firing was done in a nitrogen atmosphere in an induction furnace using a graphite susceptor. A small nitrogen flow was maintained during firing. The heating rate was 350°C/min and various holding times were used at different firing temperatures. Temperature was measured with an optical pyrometer. The specimens were furnace-cooled at a rate of ≈250°C/min to 1000°C. Further cooling to room temperature was somewhat slower.

The specimens selected for quantitative measurements were those that showed minimum weight loss when fired and that gave equilibrium phase assemblages. Equilibrium was assumed to have been attained when the number, type, and amounts of phases, as determined by XRD, did not vary with time at a fixed temperature. Equilibrium was also confirmed in some selected specimens by obtaining the same type and amounts of phases from different starting materials for a given composition. Whenever a substantial amount of liquid (> about 10%) occurred at the firing temperature, equilibrium was readily achieved, typically within 15 min.

The use of packing powder, rapid heating, and short holding time at the firing temperature kept the weight loss in the pellet at <1.5% in most cases. However, compositions containing >40 eq% O and <40 eq% Al underwent large weight losses (5 to 15%) when fired at 1750°C. Excessive weight loss did not occur at ≤ 1650°C. About 50 compositions, lying in the area above the β-ss line in Fig. 1, were fired at 1750°C to establish the isothermal section representing solid-liquid equilibria. Some selected compositions were fired at ≤ 1650°C to determine subsolidus phase equilibria and the tempera-

ture and composition of the lowest melting point. The fired specimens were examined mainly by XRD, and in some cases metallography, to determine the number and type of phases present. An automatic recording diffractometer with $CuK\alpha$ radiation at 40 kV and 15 mA was used. The samples were scanned between 10° and 80° 2θ at a rate of 2°/min. Firing conditions and phases present in various specimens after firing are given in Table I.*

Standard quantitative X-ray powder diffractometry[8] was used to determine the amount of β-ss in the selected specimens in the β-ss + liquid field to establish the tie lines in this 2-phase field at 1750°C. The specimens were ground into powder for this purpose. Calibration standards were made using 10 wt% alumina as an internal standard with different amounts of single-phase β-ss powder and silicon powder as a filler. Alumina could be used as an internal standard because the specimens in the β-ss + liquid field contained no alumina themselves. Initial trials using integrated intensities of the diffraction peaks scanned at 0.2°/min showed that no substantial improvement in the analysis was achieved by using the integrated intensities instead of the peak heights scanned at 2°/min. Therefore, the peak heights in the diffraction patterns scanned at 2°/min were taken as a measure of the concentration of a given phase in a powder mixture.

A calibration curve of the peak-height ratio vs wt% β-ss was made from the diffractometer traces of the standards. The peak-height ratio here refers to the ratio of the peak height of (301) or (321) reflection of β-ss to the peak height of (012) or (113) reflection of the internal standard α-Al_2O_3. The experimental error in determining the amount of β-ss by this method is estimated to be ± 4 wt%. The composition of β-ss in these selected specimens was determined from the change in the β-ss lattice parameters. For this purpose, a calibration curve was made[9] for lattice parameters vs eq% Al in different hot-pressed single-phase β-ss standards. The scanning rate on the diffractometer used for the lattice parameter change measurements was 0.5°/min. The basis for determining tie lines in the β-ss + liquid field from the amount and composition of β-ss in the fired specimens of this field is discussed in the next section.

III. Results and Discussion

Solid-liquid equilibria at 1750°C determined in this study are shown in Fig. 1 in equivalent percent representation.[5] At this temperature, x_1 phase is molten; evidence for this is presented later. Tie lines for the β-ss + liquid field and the corresponding part of the liquidus curve were established from the compositions and amounts of β-ss in selected specimens which had overall compositions in this 2-phase field. This derivation was possible because, during cooling from 1750°C, no significant amount of β-ss crystallized from the liquid phase as shown by the fact that compositions lying just above the liquidus curve (solid line) in the all-liquid field showed only x_1 as the crystalline phase. No β-ss was detected in these specimens by XRD. The minimum concentration of β-ss that could be detected in synthetic mixtures was 3 wt%, which means that those compositions which are totally liquid at 1750°C partially crystallized into x_1 and the rest remained as a glass and that <3 wt% β-ss precipitated during cooling.

Another feature indicating that no significant amount of β-ss crystallized during cooling in the 2-phase β-ss + liquid field is the fact that two compositions lying on the same tie line but containing significantly different amounts of liquid at 1750°C did not give different lengths of the tie line. These composition pairs are identified by the numbers 5,6; 7,16; and 8,30 (Table I). The part of the liquidus determined from the X-ray results is represented by the solid line in Fig. 1. It matches well with the melting behavior and microstructural observations. A similar determination of tie lines for the Si_2N_2O-ss + liquid field and the corresponding liquidus could not be done since liquids in this field crystallized Si_2N_2O-ss on cooling and the specimens in this field showed large weight losses by vaporization when fired at 1750°C. Therefore, the liquidus here was determined from the melting behavior and microstructural

---

*For Table I, order ACSD-143 from Data Depository Service, The American Ceramic Society, 65 Ceramic Drive, Columbus, Ohio 43214.

**Table II. Lattice Parameter Changes in Si₂N₂O Solid Solution**

Comp.				
Al (eq%)	O (eq%)	a (Å)	b (Å)	c (Å)
0	25.5	8.890	5.488	4.857
2.5	26.3	8.895	5.507	4.857
6.3	30.0	8.906	5.529	4.859

The segments of the liquidus for the mullite + liquid and the alumina + liquid fields were deduced from the phases present in the fired specimens as determined by XRD and are also shown as dashed lines. The extent of the liquid field found here is in reasonable agreement with that tentatively proposed by Layden[7] from DTA and microstructural studies. However, the shape of the liquidus is quite different, particularly for the β-ss + liquid field. This field is larger than Layden's and its liquidus curves more strongly toward the N₂-rich compositions. The solid solubility of Al in Si₂N₂O was determined from lattice parameter changes of the single-phase specimens and the appearance of secondary x_1 and β-ss phases in the neighboring compositions. The lattice parameters of Si₂N₂O-ss are given in Table II.

The composition Si₁₂Al₁₈O₃₉N₈ (i.e. 2S₃N₄·9Al₂O₃·6SiO₂) gave the highest peak intensities for the x_1 diffraction pattern and showed no other crystalline phases after firing at 1750°C. Microstructural observations showed that this composition contained less glass than any other compositions having x_1 as the only crystalline phase. Furthermore, when fired at 1650°C this composition gave x_1 phase only, whereas neighboring compositions contained secondary mullite or β-ss. Therefore, it is suggested that the stoichiometric composition of x_1 is Si₁₂Al₁₈O₃₉N₈. When heated to 1750°C, this composition spread freely in the crucible (like a melt). An optical micrograph (Fig. 2) of a polished section of this composition shows large, elongated x_1 grains, with some glass present along the grain observations alone; it is drawn as a dashed line, indicating a somewhat larger margin of error.

Some of the specimens (Nos. 10, 41, 43, and 44 in Table I) that experienced large weight losses in firing were dissolved in a borate glass made of equal weight proportions of Na₂B₄O₇ and LiBO₂. The glass samples were then analyzed for Si and Al by the electron microprobe analyzer and for N₂ content by wet chemical analysis.[10] In this analysis, NH₃ was liberated from the specimens by dissolving them in lithium hydroxide. The NH₃ liberated was determined volumetrically using standard H₂SO₄. The analyses showed that Si, N₂, and O₂ were lost by vaporization but that the Al content of the specimens increased. As a result, the overall composition shifted toward the AlN corner.
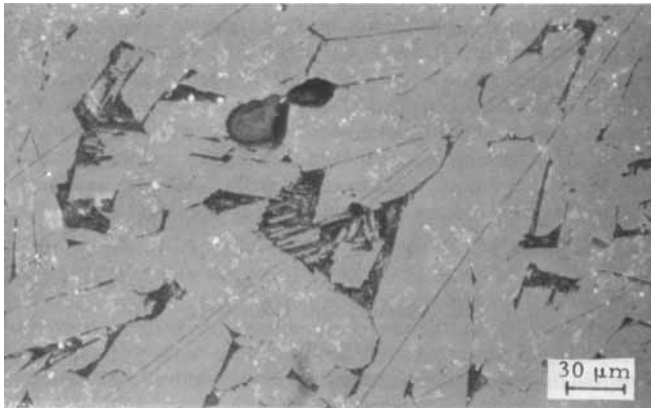
Fig. 2. Optical micrograph of polished section of 53 eq% Al-76 eq% O specimen fired at 1750°C for 10 min; HF etched.
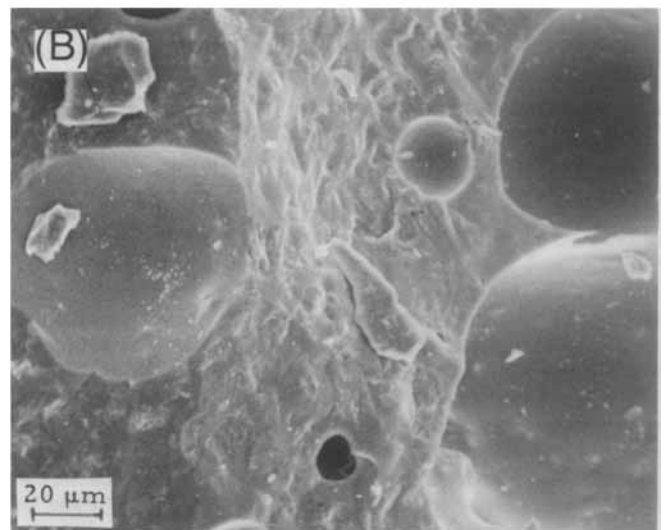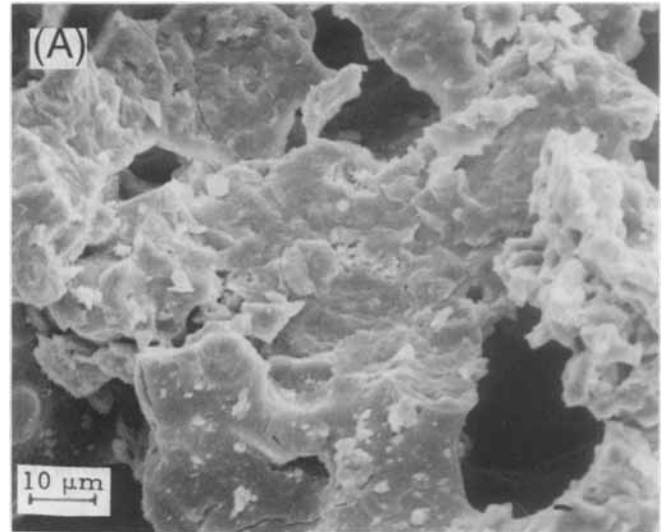
Fig. 4. Scanning electron micrographs of fracture surfaces of 10 eq% Al-90 eq% O specimen fired at (A) 1450°C for 2 h and (B) 1500°C for 2 h.
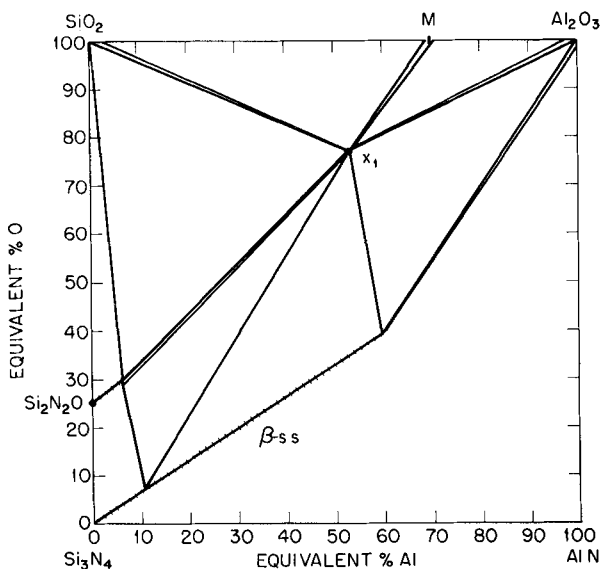
Fig. 3. Subsolidus phase equilibria; x_1 = Si₁₂Al₁₈O₃₉N₈.

boundaries. A few light-colored β-ss grains (estimated as <2 vol%) which apparently precipitated from the x_1 phase during cooling are also visible. Thus, if this is the single-phase x_1 composition, the specimen must be completely molten at 1750°C since the specimen fired at this temperature showed no other crystalline phases in the XRD pattern. The melting temperature of the x_1 phase is estimated as 1720°C. This composition lies on the line joining Si_3N_4 and mullite ($3Al_2O_3 \cdot 2SiO_2$) compositions.

Subsolidus phase equilibria in part of the system are shown in Fig. 3. The lowest-melting composition is ≈ 10 eq% Al-90 eq% O which melts at 1480°C (± 20°C). The evidence for melting in this composition is seen in the scanning electron micrographs of the fractured surfaces (Fig. 4). The specimen fired at 1450°C shows no rounded pores, whereas the specimen fired at 1500°C shows such pores which occur when densification takes place in the presence of a liquid. The appearance of the specimens and the extent of densification also indicated a large amount of liquid in the 1500°C-fired specimen and little in that fired at 1450°C.

References

[1] S. Boskovic, L. J. Gauckler, G. Petzow, and T. Y. Tien, "Reaction Sintering Forming β-Si_3N_4 Solid Solutions in the System Si,Al/N,O: I," *Powder Metall. Int.*, **9** [4] 185–89 (1977).
[2] Y. Oyama and O. Kamigaito, "Solid Solubility of Some Oxides in Si_3N_4," *Jpn. J. Appl. Phys.*, **10** [11] 1637 (1971).
[3] K. H. Jack and W. J. Wilson, "Ceramics Based on the Si-Al-O-N and Related Systems," *Nature (London), Phys. Sci.*, **238** [80] 28–29 (1972).
[4] Yoichi Oyama, "Solid Solution in the Ternary System Si_3N_4-AlN-Al_2O_3," *Jpn. J. Appl. Phys.*, **11** [5] 760–61 (1972).
[5] L. J. Gauckler, H. L. Lukas, and G. Petzow, "Contribution to the Phase Diagram Si_3N_4-AlN-Al_2O_3-SiO_2," *J. Am. Ceram. Soc.*, **58** [7–8] 346–47 (1975).
[6] P. L. Land, J. M. Wimmer, R. W. Burns, and N. S. Choudhury, "Compounds and Properties of the Si-Al-O-N System," Tech. Rept. AFML-TR-75-209, Air Force Materials Laboratory, Wright-Patterson AFB, Ohio, 1976.
[7] G. K. Layden, "Process Development for Pressureless Sintering of SiAlON Ceramic Components," Final Tech. Rept. R75-91072-4, United Technologies Research Center, East Hartford, Conn., 1976.
[8] H. P. Klug and L. E. Alexander, X-Ray Diffraction Procedures for Polycrystalline and Amorphous Materials, 2d ed.; pp. 531–62. Wiley-Interscience, New York, 1974.
[9] L. J. Gauckler, "Phase Equilibria Studies in the System Si,Al/N,O and Si,Al,Be/N,O"; Sc. D. Thesis, University of Stuttgart, Stuttgart, Federal Republic of Germany, 1976.
[10] G. Glaeser; private communication.

Hot-Pressing of Si_3N_4 with Y_2O_3 and Li_2O as Additives

L. J. BOWEN, T. G. CARRUTHERS, and R. J. BROOK*

Department of Ceramics, University of Leeds, Leeds LS2 9JT, England

The rates of densification and phase transformation undergone by α-Si_3N_4 during hot-pressing in the presence of Y_2O_3, Y_2O_3-$2SiO_2$, and Li_2O-$2SiO_2$ as additives were studied. Although these systems behave less simply than MgO-doped Si_3N_4, the data can be interpreted during the early stages of hot-pressing as resulting from a solution-diffusion-reprecipitation mechanism, where the diffusion step is rate controlling and where the reprecipitation step invariably results in the formation of the β-Si_3N_4 phase.

I. Introduction

ATTEMPTS to improve the high-temperature strength retention of hot-pressed silicon nitride[1] have included the removal of impurities present in the starting materials, especially Ca, Na, and K, which concentrate in the glassy grain-boundary phase[2] and lower its softening point,[3] and the choice of an additive which aids densification and forms a refractory grain-boundary phase. One additive which satisfies this requirement is yttrium oxide.[4]

The role of yttria in aiding densification is not fully understood. Gazza[5] reported that, to obtain rapid densification and the strongest material, 5 to 10 wt% Y_2O_3 additive is needed, whereas typical levels are 1 to 3 wt% for the magnesia additive used in commercially manufactured hot-pressed silicon nitride. Densification measurements made at 1450° to 1650°C showed that the rate of densification was linear up to 0.70 to 0.80 relative density (ρ), which was attributed to particle rearrangement accompanying the reaction between the additive and either the silicon nitride or the silica films present on the surfaces of the nitride crystallites. X-ray diffractometry (XRD) studies on cold compacts prepared at higher temperatures (up to 1750°C) revealed the presence of crystalline second phases, possibly yttrium silicates formed at the hot-pressing temperature.

Several attempts have been made to determine the structure and composition of these second phases.[4-9] Wills[6] proposed that a densification-enhancing liquid of composition $Si_3N_4 \cdot 3Y_2O_3$ formed at hot-pressing temperatures up to 1700°C and then reacted with more silicon nitride to produce highly refractory $Si_3N_4 \cdot Y_2O_3$, thus imparting improved high-temperature strength and creep properties to the material. Tsuge et al.[7] also identified a crystalline phase of composition $Si_3N_4 \cdot Y_2O_3$ in hot-pressings prepared at >1750°C and tentatively postulated the existence of another second phase of composition $Si_3N_4 \cdot 2Y_2O_3$. Two other yttrium silicon oxynitride compounds (compositions $Si_3N_4 \cdot 9SiO_2 \cdot 10Y_2O_3$ and $Si_3N_4 \cdot SiO_2 \cdot 4Y_2O_3$) have been isolated.[8,9]

In view of the technological importance of hot-pressed yttria-doped silicon nitride for high-temperature engineering applications, it is desirable to understand more fully the mechanisms of densification and of the simultaneous α-β phase transformation[10] in this material. The present work aims to achieve such an understanding by investigating the hot-pressing and transformation behavior of yttria-doped silicon nitride and by comparing this behavior with that of magnesia-doped and lithia-doped silicon nitride.

II. Experimental Procedure

(1) Equipment

Details of the apparatus and procedures used for hot-pressing have been described elsewhere.[10] For the phase transformation studies, the α:β silicon nitride ratios were measured by XRD with Ni-filtered Cu$K\alpha$ radiation, using a calibration procedure[11] based on measurements of the ratio of intensities of the α_{102} and β_{210} reflections.

(2) Materials Characterization and Additive Preparation

The silicon nitride powder used throughout the present work was identical to that used in a previous study with MgO as additive.[10,12] The powder,* which contained 94 wt% α phase, was prepared from

*Allen Clarke Research Laboratories, Towcester, Northamptonshire, United Kingdom.